PIC modeling challenges in diverse low temperature plasma scenarios

Filippo Cichocki[(*)1], Vittorio Sciortino[2], Pierpaolo Minelli[3], Francesco Taccogna[3]

[1] *ENEA, C.R. Frascati, Dipartimento "Nucleare" (NUC), Frascati, Italy*
[2] *Università "Aldo Moro", Dipartimento di Fisica, Bari, Italy*
[3] *Institute for plasma science and technology (ISTP), Bari, Italy*
[(*)] filippo.cichocki@enea.it

Particle-in-cell modeling is particularly appropriate to study the complex kinetics of low temperature plasmas. In this work, we present a few challenges in PIC modeling for low temperature plasmas, with a direct application in 3 different scenarios: the plasma discharge inside a negative ion source, the plasma interaction with a fusion reactor monoblock, and the collisionless expansion of a propulsive plasma within a magnetic nozzle. These examples will serve to highlight the high versatility of the PIC modeling approach and to illustrate the different solutions adopted in each case.

1 Introduction

The particle-in-cell method [1], complemented with Monte Carlo collisions algorithms for volumetric collisions and other phenomenological models to account for plasma-wall interaction phenomena, represents a very flexible and adaptable approach to deal with a large variety of low temperature plasma scenarios, and especially with those featuring a complex non-equilibrium kinetics. This work focuses on electrostatic PIC models, in which the set of considered Maxwell's equations reduces to Poisson's equation and a time-constant non-uniform magnetic induction field is assumed. The peculiarities and challenges of the PIC approach in 3 different application scenarios are then discussed in detail: (i) a negative ion source, where special care is given to the description of the collisional processes and of the electron energization, (ii) the simulation of the plasma-wall interaction at a fusion reactor monoblocks, where specific plasma-wall interaction models are implemented, and, finally, (iii) the expansion of a propulsive plasma within a magnetic nozzle with a focus on the correct outflow boundary conditions.

2 Simulation of a negative ion source

Negative ion sources [2] are characterized by a relatively low dense - low temperature plasma, with plasma densities in the order of $10^{18}\mathrm{m}^{-3}$ and electron temperatures of a few tens of eV. The magnetic filter used to prevent electrons from reaching the extraction region has the effect of enhancing their non-Maxwellian behaviour, so that a kinetic treatment is particularly needed. Here, we have applied the PICCOLO code ("PIC COde for LOw temperature plasmas") to model the plasma generation and transport within SPIDER [4], the negative ion source currently considered for the ITER fusion reactor. Two aspects are worth a special discussion: the electron energization, and the collisional processes.

Regarding the former, in SPIDER, the plasma is heated by 8 RF drivers with a cylindrical shape (see Fig. 1, which shows only 4 drivers, being a 2D $y-z$ simulation). Since the implemented PIC model is electrostatic, no direct interaction between electrons and RF fields is simulated, therefore an alternative energization algorithm is implemented to mimic the correct energy absorption [5]. At each PIC step, given the total absorbed power P_{abs} per driver, the heating RF frequency f_{RF}, the average kinetic energy $\langle E_{\mathrm{k}}\rangle$ of electrons and the total number of electron macro-particles $N_{\mathrm{mp,tot}}$ within each driver, a target heating temperature is computed as:

$$T_{\mathrm{heat}} = \frac{2}{3}\left(\langle E_{\mathrm{k}}\rangle + \frac{P_{\mathrm{abs}}}{eN_{\mathrm{mp,tot}}W_{\mathrm{mp}}f_{\mathrm{RF}}}\right), \tag{1}$$

where W_{mp} represents the number of elementary electrons per macro-particle. Then, if Δt_{PIC} is the PIC time step, a given number of electrons $N_{\mathrm{mp,heat}} = f_{\mathrm{RF}}\Delta t_{\mathrm{PIC}}N_{\mathrm{mp,tot}}$ inside each driver is randomly selected and their velocity resampled from a Maxwellian velocity distribution, with temperature T_{heat}.

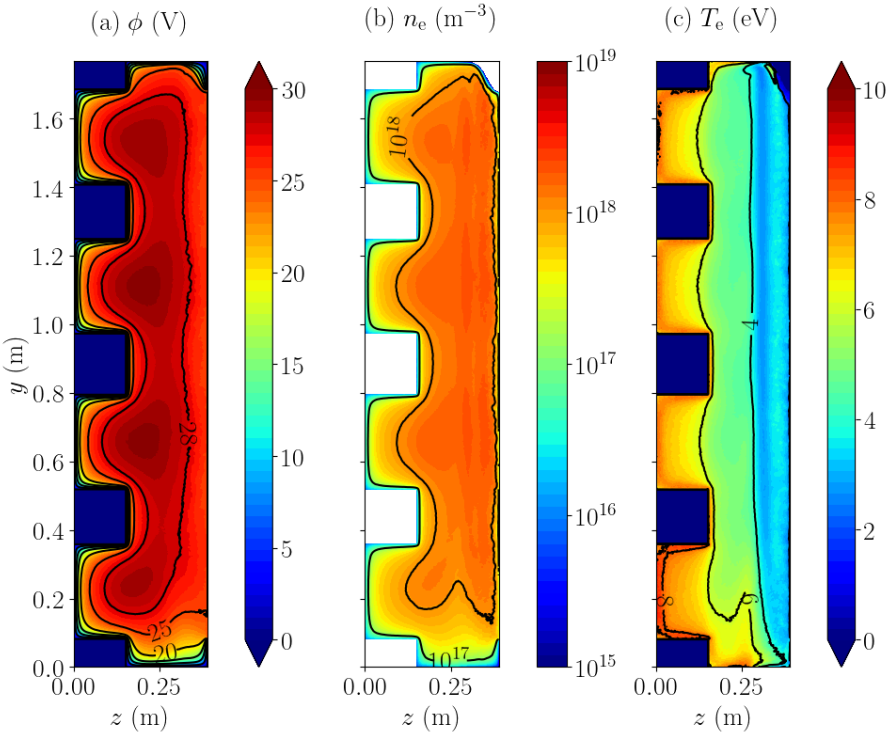

Fig. 1: (a) Plasma potential, (b) plasma density and (c) electron temperature in a 2D simulation of the SPIDER negative ion source. The domain is uniform in the direction normal to the page (x). The magnetic induction field is perpendicular to the page and peaks to 7 mT close to the extraction grid ($z_{\max}$).

Volumetric collisions are modeled with a Monte Carlo Collisions technique [3], based on the "Null Collisions" method. The neutral gas is considered here as a fixed uniform background and consists in a mixture of hydrogen molecular and atomic gas (of density around $2 \cdot 10^{19}$ m^{-3}). A large set of collisional processes are included, and namely ionization, elastic, and excitation collisions, but also (for the molecular gas) dissociation, dissociative ionization, and dissociative attachment (that leads to a negative hydrogen ion). For what concerns wall interaction, on the other hand, the simulation of the emitted negative ion current would require to model the emission of negative ions from the caesiated molybdenum extraction grid, due to both neutral atom and ion impacts [2]. However, this has not been included in the simulations where no negative ions are tracked.

Referring to Fig. 1, a simplified 2D geometry has been considered, with 4 drivers featuring $P_{\text{abs}} = 100$ kW and assumed to be uniform along the x direction. Homogeneous Dirichlet conditions are imposed at the drivers and expansion chamber walls ($\phi = 0$ V), while a slightly positive potential (25 V) is imposed at the extraction grid surface ($z = z_{\max}$). Finally, a vacuum permittivity ϵ_0 increased by a factor of 22500 is applied to reduce the computational cost. This has the effect of increasing the width of plasma sheaths by a factor of 150, however, the transport within the acceleration chamber and the collisional processes in the volume are correctly reproduced.

3 Plasma-wall interaction at the divertor monoblocks

Magnetic confinement tokamak reactors are designed to divert a significant fraction of the power exhaust towards a dedicated wall (named divertor) that is made of many small monoblocks (with a characteristic size of 1 cm and typically made of tungsten). The assessment of the energy and particle fluxes on the walls is therefore crucial, and it has already been attempted with a PIC model, considering a realistic monoblock geometry for the DTT reactor [6]. In this scenario, it is particularly relevant to include in the modeling (apart from collisional processes with the neutral background) also the physics of the plasma-wall interaction. In this respect, the most relevant phenomena are secondary electron emission (SEE)

from electron impacts (which is around 1 order of magnitude larger than that induced by ions), and, given the large operating monoblock temperatures (> 2000 K), also the thermionic electron emission. Here, the models presented in Ref. [7] have been considered, and SEE electrons are divided between backscattered electrons and true secondaries, since these two sub-populations can have very different emission energy and angle distributions.

Some preliminary results from the project PARADIGM ("PARametric Analysis of DIvertor Geometry considering Multiple kinetic effects") obtained with the DESPICCO code ("Divertor Edge Simulator of Plasma-wall Interaction with Consistent COllisions") are shown in Fig. 2. A Deuterium plasma and background gas are considered with real elementary particle masses, in a 2D domain extending along the toroidal direction y and the direction normal to an axisymmetric divertor z. Periodic conditions for both particles and fields are assumed at $y_{\min}, y_{\max}$ (see Ref. [7] for more details). The main goal is to assess the effect of the monoblock geometry and of the plasma and magnetic field conditions, on the energy fluxes to the walls. Fig. 3 shows the 2D potential and electron density maps in two scenarios featuring different monoblock geometries and magnetic field orientations. Electron surface emission (mainly due to thermionic emission) can be appreciated in subplot (a) close to the monoblock surface.

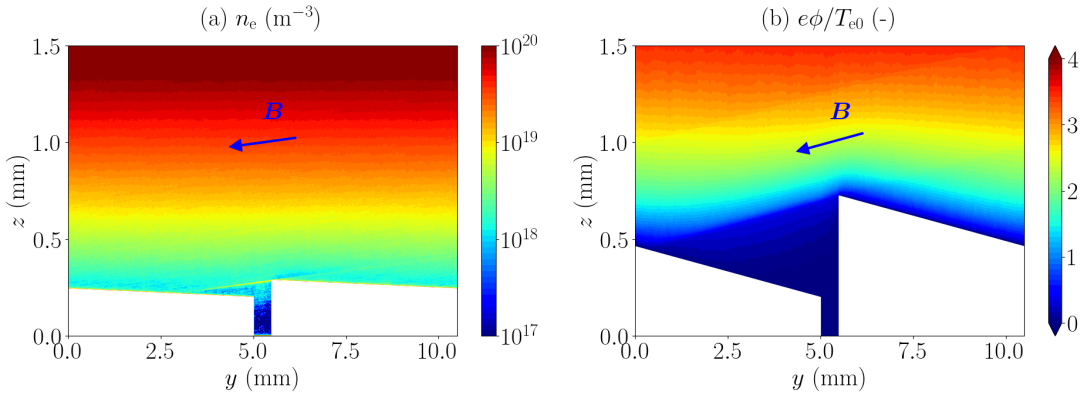

Fig. 2: (a) Electron density and (b) normalized electric potential ($T_{e0} = 40$ eV) for an angle of (a) 2 deg and (b) 6 deg between $\boldsymbol{B}$ (shown by a blue arrow) and the bevelled monoblock surface. Thermionic electron emission with a wall temperature of 3300 K is assumed here.

4 Magnetic nozzle simulation

Magnetic nozzles (MNs) are convergent-divergent magnetic field topologies used in electric thrusters to guide the plasma ions acceleration downstream. While the issue of the ion streamlines detachment appears to have been properly explained with a 2-fluids model [8], there are still many open aspects in the study of this technology that require a fully kinetic treatment, such as the non-equilibrium electron thermodynamics and the electron streamlines detachment.

A subtle and relevant topic in MNs simulation is that of the particle boundary conditions at the open outflow boundaries, a topic that has already been treated by several authors [9, 10]. Since electrons are much more mobile than ions, when the plume reaches the downstream boundary, a much larger number of electrons would get lost because of their much larger mobility, so that some of them must be reflected backwards to guarantee a globally ambipolar plume. Fig. 4 shows some preliminary results for a typical MN expansion obtained with the PICCOLO code, and assuming an artificially increased vacuum permittivity (by a factor of 1000) to limit the computational cost. In the simulation, we impose a fixed flux of electrons and Xe ions (with their real elementary masses) from the leftmost domain boundary ($z = 0$). Quasi-neutrality is automatically satisfied by refluxing all particles that cross the injection surface (at $z = 0$) towards the source plasma ($z < 0$). At the open boundaries $z_{\max}$ and $r_{\max}$, on the other hand, all ions are lost and electrons are either reflected or not, according to their mechanical energy E_{tot} (relative to infinity),

$$E_{\text{tot}} = \frac{1}{2} m_e v_e^2 - e\left(\phi_{\text{exit}} - \phi_{\text{infty}}\right), \tag{2}$$

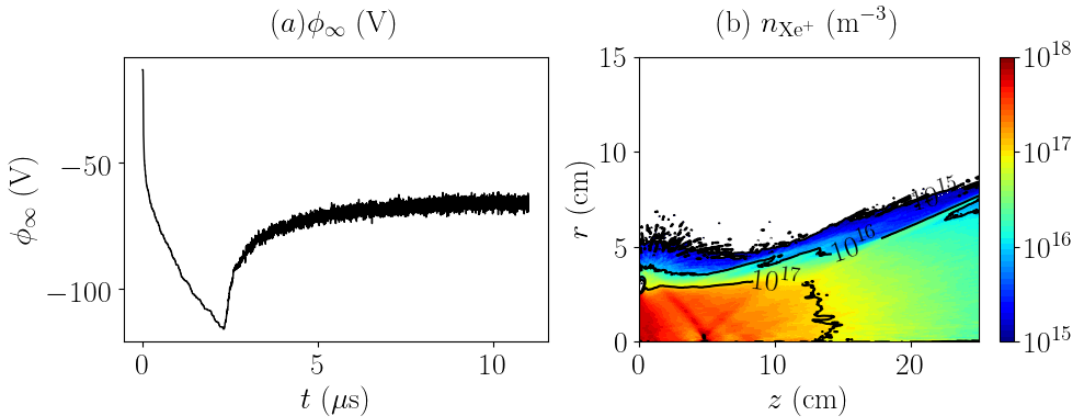

Fig. 3: (a) Time evolution of the infinity potential ($\phi = 0$ at $r = z = 0$), and (b) Xe ion density 2D map. The domain is cylindrical, with $r = 0$ corresponding to the plume centerline.

where m_e, v_e are the elementary electron mass and velocity, ϕ_{exit} is the local electric potential at the outflow position, and ϕ_{infty} is the potential at infinity. All electrons with $E_{tot} < 0$ are specularly reflected backwards toward the simulation domain, while all ions and electrons with $E_{tot} > 0$ are lost and charge up a virtual capacitor at infinity, according to:

$$\frac{d\phi_\infty}{dt} = \frac{I_i + I_e}{C_\infty}, \tag{3}$$

where I_i, I_e are the ion and electron currents that leave the domain, and C_∞ is an equivalent electric capacity. As shown in Fig. 4(a), the capacitor at infinity charges up negatively with respect to the plasma plume, and when it reaches a stationary value, current ambipolarity is guaranteed, with no boundary effects on the plasma plume properties, as shown in Fig. 4(b).

5 Conclusions

The increasing computational power of modern High Performance Computing clusters, makes the PIC modeling approach more and more convenient for an ever growing range of applications and scenarios. This work has highlighted such a high versatility by presenting and discussing three plasma scenarios featuring different numerical and physical challenges.

Acknowledgments

The simulations of Sec. 3 have been run as part of the PARADIGM Eurofusion HPC project, on the Marconi and LEONARDO HPC clusters.

Bibliography

[1] F. Taccogna, F. Cichocki *et al*, J. Appl. Phys. **134** (2023) 150901.
[2] M. Bacal, *Physics and applications of hydrogen negative ion sources*, Springer Nature **124**, 2023
[3] V. Vahedi and M. Surendra, Computer Physics Communications **87** (1-2) 179-198, 1995
[4] G. Serianni *et al*, Fusion Engineering and Design **146** 2539–2546, 2019
[5] G. Fubiani, L. Garrigues *et al*, New Journal of Physics, **19** 015002, 2017
[6] F. Cichocki, P. Innocente *et al*, Plasma Phys. Control. Fusion **66** 025015, 2024
[7] F. Cichocki, V. Sciortino *et al*, Nucl. Fusion **63** 086022, 2023
[8] M. Merino and E. Ahedo, Plasma Sources Sci. Technol. **23** 032001, 2014
[9] S. Andrews, S. Di Fede and M. Magarotto, Plasma Sources Sci. Technol. **31** 035022, 2022
[10] M. Li, M. Merino *et al*, Plasma Sources Sci. Technol. **28** 034004, 2019